Biophysical Chemistry 193–194 (2014) 27–34

Contents lists available at ScienceDirect

Biophysical Chemistry

journal homepage: http://www.elsevier.com/locate/biophyschem

α-Lactalbumin nanoparticles prepared by desolvation and cross-linking: Structure and stability of the assembled protein

Izlia J. Arroyo-Maya [a,b,*], Humberto Hernández-Sánchez [c], Esmeralda Jiménez-Cruz [c], Menandro Camarillo-Cadena [b], Andrés Hernández-Arana [b,**]

[a] Department of Food Science, University of Massachusetts, Amherst, MA 01003, USA
[b] Área de Biofisicoquímica, Departamento de Química, Universidad Autónoma Metropolitana-Iztapalapa, Apartado Postal 55-534, Iztapalapa, D.F. 09340, Mexico
[c] Departamento de Graduados e Investigación en Alimentos, Escuela Nacional de Ciencias Biológicas, Instituto Politécnico Nacional, Carpio y Plan de Ayala, Miguel Hidalgo, D.F. 11340, Mexico

HIGHLIGHTS

- Desolvation and cross-linking of bovine α-lactalbumin yield spheroidal nanoparticles.
- During the assembly process α-lactalbumin acquires a β-strand-like conformation.
- Nanoparticles contain a low protein weight-fraction.
- At low temperature, nanoparticles are stable in the 3.0–9.0 pH region.
- Non-covalent interactions contribute to the thermal stability of nanoparticles.

GRAPHICAL ABSTRACT

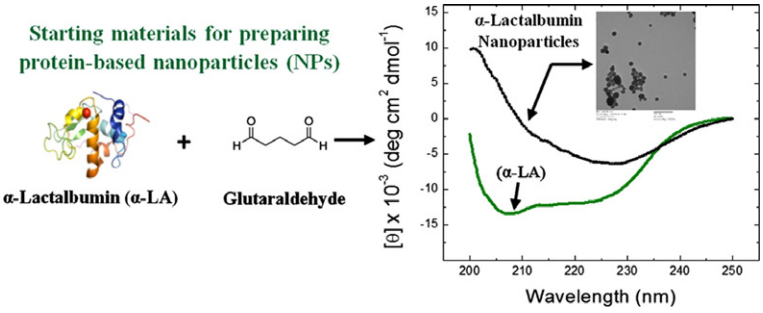

ARTICLE INFO

Article history:
Received 7 June 2014
Received in revised form 16 July 2014
Accepted 16 July 2014
Available online 27 July 2014

Keywords:
α-Lactalbumin
Nanoparticles
Secondary structure
Circular dichroism
Differential scanning calorimetry

ABSTRACT

A key step in the preparation of cross-linked protein nanoparticles involves the *desolvation* of proteins with an organic solvent, which is thought to act by modulating hydrophobic interactions. However, to date, no study has examined the conformational changes that proteins undergo during the assembly process. In this work, by using several biophysical techniques (CD spectroscopy, DSC, TEM, etc.), we studied spheroidal nanoparticles made from bovine α-lactalbumin cross-linked with glutaraldehyde in the presence of acetone. Within the nanoparticle, the polypeptide chain acquires a β-strand-like conformation (completely different from the native protein in secondary and tertiary structure) in which several side chains likely become available for reacting with glutaraldehyde. A multiplicity of cross-linking sites, together with the polymeric nature of glutaraldehyde, may thus explain the low dry-weight fraction of protein that was found in the nanoparticles. Although covalent bonds undoubtedly constitute the main source for nanoparticle stability, noncovalent interactions also appear to play a role in this regard.

1. Introduction

Protein-based nanoparticles are currently under extensive investigation due to their potential applicability in the pharmaceutical and food industries. In principle, protein nanoparticles are biodegradable, non-antigenic, metabolizable and easily modifiable for surface alterations and the covalent attachment of other molecules [1]. All of these characteristics make these protein-derived materials suitable for use

* Correspondence to: I.J. Arroyo-Maya, Área de Biofisicoquímica, Departamento de Química, Universidad Autónoma Metropolitana-Iztapalapa, Apartado Postal 55-534, Iztapalapa, D.F. 09340, Mexico. Tel.: +1 413 5457157; fax: +1 413 5451262.
** Corresponding author. Tel.: +52 55 58044674; fax: +52 55 58044666.
E-mail addresses: iarroyo@foodsci.umass.edu (I.J. Arroyo-Maya), aha@xanum.uam.mx (A. Hernández-Arana).

http://dx.doi.org/10.1016/j.bpc.2014.07.003
0301-4622/

as carriers for bioactive compounds found in foods, such as peptides, vitamins, and antioxidants [2–4]. Furthermore, nanoparticles may improve the water solubility, thermal stability and oral availability of a number of compounds [5–8].

The size and hydrophilic–hydrophobic surface balance characteristics are two main physicochemical properties that allow protein nanoparticles to achieve an adequate biodistribution and the consequent site-specific delivery of bioactive compounds. With regard to particle size, particles should be small enough to not be removed by intestinal clearance mechanisms. Because nanoparticles are characterized by a solid particle matrix, these systems are capable of remaining in the circulatory system for longer periods when their size ranges between 100 and 200 nm [9].

The protocols used to prepare protein nanoparticles can be classified in two main techniques: emulsification and desolvation. Emulsification methods have the disadvantage of requiring large amounts of organic solvents for the removal of the lipid residues and emulsifiers used in the process. A good alternative for preparing protein-based nanoparticles is the desolvation method, which is derived from the coacervation method of microencapsulation [1,10]. This method takes advantage of the desolvation that occurs upon the addition of agents, such as alcohol, acetone or inorganic salt, at high concentrations. This addition normally leads to coacervation, and microcapsules are formed by this process. However, if the addition of the desolvating agent is stopped shortly before phase separation occurs, the molecules, which are thought to have a tightly packed conformation, can be cross-linked with glutaraldehyde, thus leading to the formation of stable nanoparticles [11]. Up to date, the desolvation method has been used to prepare nanoparticles of human serum albumin [12], bovine serum albumin [13], bovine β-lactoglobulin [5], and bovine α-lactalbumin [14,15].

As described in the literature [1,15,16], a successful strategy for obtaining size-controlled nanoparticles with a narrow size distribution requires the careful control of several parameters, such as the type of desolvating agent, the pH of the protein solution, protein and organic solvent concentrations, the rate and manner in which the organic solvent is added, the stirring rate of the protein solution during the desolvation process, and the cross-linker-to-protein concentration ratio. Organic solvents that have been used for desolvation (i.e., acetone, ethanol, and isopropanol) are thought to act as modulators of intermolecular hydrophobic interactions, thus controlling the number of protein molecules that can be assembled and the size of the resulting particles [17]. However, it is well-known that organic solvents, when present at high concentrations, induce large conformational changes in proteins because they promote the exposure of internal nonpolar groups to the water–organic solvent mixture [18,19]. This notwithstanding, no studies have addressed the conformational changes proteins undergo during the assembly process or the actual composition of cross-linked-protein nanoparticles.

In this study, we have performed spectroscopic and calorimetric studies aimed at disclosing the basic structural characteristics of bovine α-lactalbumin (α-LA), as assembled by glutaraldehyde cross-linking in the presence of acetone. α-LA is an acidic, single chain Ca^{2+}-binding protein composed of 123 amino acids and four disulfide bonds, the native structure of which has a predominantly α-helical conformation. This is the second most abundant protein in whey, making up 20% (w/w) of the total protein content. α-LA is easily isolated from sweet dairy whey (a by-product of cheese making) in a relatively pure form, which makes it a promising starting material for preparing *nanocarriers* for bioactive compounds. α-LA nanoparticles were assembled as previously reported [5,9,15]. Their characterization first included the precise quantification of the protein incorporated into the nanoparticle matrix, which was an essential step for obtaining meaningful results from spectroscopic and calorimetric methods. Circular dichroism spectra revealed that the polypeptide chain of assembled α-LA displays a β-strand-like conformation devoid of the tertiary structure of the native protein. In this conformation, which appears to be induced by the high acetone concentration used in the assembly process, many α-LA side chains are likely capable of reacting with glutaraldehyde, thus leading to the formation of 100–160 nm diameter nanoparticles with a low dry-weight content of protein. In addition, although nanoparticles are mainly stabilized by covalent bonds, calorimetric scans indicated that interactions of a noncovalent origin also contribute to the stability of these assemblies.

2. Experimental section

2.1. Materials

BioPURE α-lactalbumin (α-LA) (production batch JE 005-8-410) was kindly donated by Davisco Foods International Inc. (Eden Prairie, MN). The composition of the sample provided by the supplier was as follows: moisture content, 5.5%; protein, 95% (91% of the protein corresponded to α-LA); fat, 0.5%; carbohydrates, 0.5%; and ash, 2.5%. All other reagents were purchased from Sigma-Aldrich (St. Louis, MO), J.T. Baker (Phillipsburg, NJ); they were of analytical grade and used as received.

2.2. Methods

2.2.1. Preparation of α-LA nanoparticles

The α-LA nanoparticles (hereafter referred to as NPs) were prepared according to a previously reported procedure [9,12], which is based on the desolvation technique described by Marty et al. [20]. Briefly, α-LA (40 mg) was dissolved in 2.0 mL of a 10 mM NaCl solution at pH 9.0 followed by the desolvation of the protein in solution by the controlled (1.0 mL min^{-1}) dropwise addition of 8.0 mL of the desolvating agent (acetone) with constant stirring (500 rpm). Immediately after the desolvation step, 40 μL of 8% aqueous glutaraldehyde solution was added to achieve α-LA cross-linking. After stirring for 3 h, the resulting nanoparticles were purified by 5 cycles of centrifugation (25,000 ×*g*, 30 min, 4 °C), and the pellet was redispersed in a 10 mM NaCl solution (pH 9.0) in the original volume by ultrasonication in a bath-type sonicator. All preparations were performed at room temperature (25 °C).

2.2.2. Determination of the protein assembled in nanoparticles

The amount of α-LA assembled into nanoparticles was directly determined after the purification step by three different methods: the determination of the total nitrogen released as ammonia by the Kjeldahl digestion, the bicinchoninic acid (BCA) assay, and the UV absorbance as corrected by light scattering.

The Kjeldahl method was carried out using a Block Digester/Steam Distiller apparatus (Labconco, Kansas City, MO), according to the AOAC official method 991.20 [21]. In summary, an appropriate volume of nanoparticle suspension was digested in concentrated H_2SO_4 using K_2SO_4 and $CuSO_4 \cdot 5H_2O$ as catalysts. The released ammonia was collected in a solution with an excess of H_3BO_3, and the ammonium ion formed was quantitated by titration with HCl. From the amount of nitrogen found in the sample, the protein mass was computed by means of the weight percent of nitrogen in α-LA.

For the BCA protein assay [22], which relies on the reduction of Cu^{2+} ions by the peptide groups in proteins and the subsequent formation of a purple-colored complex composed of Cu^{+1} and bicinchoninic acid, we used the Pierce BCA Protein Assay Kit 23225 (Thermo Fisher Scientific Inc., Rockford, IL). An aliquot of the nanoparticle suspension (50 μL) was diluted with 950 μL of 10 mM NaCl (pH 9.0). To 50 μL of the diluted suspension, 1000 μL of the working reagent was added. After incubating the reaction mixture at 60 °C for 15 min, the sample absorbance was measured at 562 nm, and the protein content was calculated from a previously prepared α-LA standard curve.

The dry matter contained in a suspension of nanoparticles was determined by means of a thermobalance (Mettler-Toledo Inc., Columbus,

OH). Five milliliters of the suspension was transferred to a crucible and dried to constant weight. From these determinations, the mass of protein per gram of the total nanoparticle solids was calculated.

Attempts were also made to directly estimate the concentration of α-LA in the suspension of nanoparticles from its UV-absorption spectrum. This well-known method is simple and reliable provided that the protein solution contains no major contaminants and does not scatter a significant fraction of the incident radiation. However, due to the large size of the α-LA nanoparticles, a suspension of these particles is expected to scatter radiation in all directions, thus causing an apparent absorption in the direction of the incident light beam [23]; furthermore, in Rayleigh's approximation (i.e., when the light wavelength is longer than the wavelength at which the absorption bands occur), the intensity of scattered light is inversely proportional to the fourth power of the wavelength. Accordingly, we corrected the observed nanoparticles UV–Vis absorption spectrum by subtracting the approximate scattering *absorption* curve, which was assumed to obey the relationship [23]:

$$A\,(scattering) = a + b(\lambda^{-n}).$$

The above equation was fitted to spectral data in the range of 350–600 nm to obtain the empirical coefficients, *a*, *b*, and *n*. In the aforementioned range (where true absorption bands are not expected), the absorption of the experimental nanoparticle spectra only showed a monotonic absorption increase as λ decreased (with *n* values close to three), thus indicating that scattering correction may work for an approximate estimation of assembled protein. From the scattering-corrected spectra, the concentration of α-LA was calculated using the extinction coefficient of the protein at 280 nm (28,616 M^{-1} cm^{-1}).

2.2.3. Spectroscopic studies

2.2.3.1. Circular dichroism. Conformational changes occurring once the protein was assembled into nanoparticles were monitored by circular dichroism (CD) spectroscopy. CD spectra were registered in a J-715 spectropolarimeter (JASCO, Easton, MD) equipped with a PTC-348WI Peltier-type holder for temperature control and magnetic stirring. The secondary structure of the assembled and native α-LA was assessed from spectra registered over the 200–250 nm (far-UV) range. Measurements were made in a 1.00-cm cuvette with α-LA solutions (15 μg mL^{-1}) or a diluted suspension of nanoparticles containing 30 μg of protein per milliliter. The registration of spectral data was stopped when the high-tension voltage in the detector reached 750 V. All samples were previously equilibrated against the appropriate buffer (50 mM sodium phosphate, pH 7.0; 10 mM sodium acetate, pH 3.0; and 10 mM sodium borate, pH 9.0). Low-temperature spectra were obtained at 25 °C from freshly prepared samples. These samples were heated up to 90 °C (maximal temperature reached with our experimental setup) and let stand at this temperature for 10 min, after which the high-temperature spectra were registered. Tertiary structure changes were evaluated in the near-UV spectral region (250–330 nm), using protein concentrations ca. 1.0 mg mL^{-1}. The results are reported as mean residue ellipticity.

2.2.3.2. Intrinsic fluorescence. The polarity of the microenvironment around tryptophan residues was investigated by measuring the intrinsic fluorescence of α-LA and α-LA nanoparticles after sample excitation with 280 nm UV radiation. Emission spectra were registered from 290 to 500 nm in a K2 spectrofluorometer (ISS Inc., Champaign, IL) with 1.00-cm cells. Nanoparticle and monomeric α-LA samples were equilibrated in the same buffer solutions used for DC studies, and the protein concentration was adjusted to 50 μg mL^{-1}.

2.2.4. Protein nanoparticle size and distribution

The size distribution of α-LA nanoparticles was analyzed by dynamic light scattering (DLS) using a Zetasizer Nano ZS90 (Malvern Instruments Ltd., Malvern, UK). This technique, which is extensively used as an adequate means to measure particle sizes over the range of a few nanometers up to 1 or 2 μm, allowed for the determination of the hydrated-nanoparticle apparent size (hydrodynamic diameter). Nanoparticle samples were diluted 1:400 with deionized water and filtered through 0.22-μm membranes immediately before use. Samples were placed in a quartz cell and equilibrated to 25 °C. Typically, 3 measurements of 60 s each were collected at a scattering angle of 90°. The hydrodynamic radius was calculated with Zetasizer Nano ZS90 software.

2.2.5. Transmission electron microscopy

The morphology of the nanoparticles was analyzed with a JEM1010 transmission electron microscope (JEOL, Tokyo, Japan) at a voltage of 60 kV. The aqueous dispersion of the nanoparticles was diluted 10 times, and 5 μL was drop-casted onto a formvar carbon-coated copper grid (200 mesh); the grid was air-dried at room temperature before loading into the microscope. Images of α-LA nanoparticles were photographically recorded in randomly selected fields at several instrumental magnifications using tools in the microscope software.

2.2.6. Calorimetric studies

2.2.6.1. Differential scanning calorimetry. Differential scanning calorimetry (DSC) was employed to monitor the heat effects originating from structural changes induced by increasing the temperature of nanoparticles in suspension. DSC experiments were performed on a differential scanning nanocalorimeter (Nano DSC 6300; TA Instruments-Waters LLC) equipped with 0.300-mL capillary cells. Nanoparticle samples (containing 2.0–4.0 mg of protein per milliliter) and buffer reference solutions were properly degassed and carefully loaded into the calorimeter cells to avoid bubble formation. Both cells were pressurized to nearly 3.0 atm and equilibrated before heating was performed at a constant rate of 1.0 °C min^{-1}. To achieve a near perfect baseline repeatability, approximately ten reference scans with buffer-filled cells preceded each sample run. Samples were routinely scanned twice to assess the reversibility of any heat effect observed on a first run. The software package provided by the manufacturer was used for data analysis, including baseline subtraction, calculation of specific heat capacity, and determination of enthalpy changes.

3. Results

3.1. Determination of protein content

As described in our previous study [15], α-LA nanoparticles (NPs) assembled by cross-linking with glutaraldehyde in a solution containing 80% acetone had an average size of ca. 150 nm with a narrow size distribution. To further characterize the properties of the protein incorporated into nanoparticles it is necessary to precisely determine the protein content in the nanoparticle suspension. Therefore, samples of NPs (prepared as described in the Experimental section) were analyzed by three different methods: direct determination of total nitrogen by the Kjeldahl method, BCA assay, and UV absorbance, corrected for scattering. As determined by the Kjeldahl method (which is regarded as the most accurate method because all the nitrogen in the NPs should come from the protein), the amount of α-LA incorporated was 2.0 ± 0.7 mg per milliliter of the final nanoparticle suspension (average of three individual batches of NPs), which is equivalent to 40 mg per gram of total solids. The BCA assay indicated a similar protein content of 2.3 ± 0.8 mg mL^{-1}. However, for an individual batch, the precision achieved by the Kjeldahl and BCA assays was ±0.06 and ±0.01 mg mL^{-1}, respectively. The overall yield, calculated as the amount of assembled α-LA with respect to the total protein used for the cross-linking process, was approximately 54%. Similar yields have been reported for the preparation of human serum albumin nanoparticles [9,10].

In contrast, scattering-corrected UV-absorption measurements resulted in a higher protein contents (3.2 ± 0.4 mg mL^{-1}, average of three nanoparticle preparations) than those determined by the other two methods. In addition, UV-absorption determinations were less precise (i.e., ±0.20 mg mL^{-1}). There is, indeed, an intrinsic difficulty in estimating the protein content by light absorption, as can be observed in the UV-absorption spectrum of NPs (Fig. 1). Specifically, the absorption bands located between 274 and 291 nm, which arise from tryptophan and tyrosine residues, are barely discernible in the intense, monotonic background due to light scattering. In view of the above results, the BCA assay (which gave results similar to the Kjeldahl method and was more easily performed) was used in further studies.

3.2. Conformational changes in α-LA upon the formation of nanoparticles

The far-UV CD spectrum of α-LA NPs (pH 7.0) displayed a broad negative band centered on 226 nm (Fig. 2a, dotted line). Because control polymerized glutaraldehyde samples gave a flat ellipticity trace (see inset in Fig. 2a), the CD band observed with the NPs can be attributed to the protein present therein. The overall characteristics (i.e., peak position and ellipticity magnitude) of the NP spectrum resemble those found in proteins with a high content of β-strands [24,25]. In contrast, the CD spectrum of native α-LA in aqueous buffer (solid curve in Fig. 2a) clearly reflects the large number of α-helix regions found in this macromolecule [26,27]. These results indicate that α-LA suffers large conformational changes in its secondary structure upon desolvation and cross-linking. Such a qualitative description was confirmed by spectral deconvolution, the results of which (Table 1) are consistent with an increase of ca. 35% of β-strand and a decrease of 26% of α-helix when the protein is incorporated into nanoparticle assemblies.

In the near-UV region, the typical CD signals of α-LA [27] were found to be absent in the NP spectrum (Fig. 2b), thus suggesting that a drastic change in the tertiary interactions surrounding tyrosine and tryptophan residues occurs during the assembly. This finding was expected, since the tertiary structure of proteins is more sensitive to alterations in the physical environment than the secondary structure. Furthermore, the emission spectrum of NPs (pH 7.0) showed a broad band centered on approximately 318 nm, which likely originated from the intrinsic fluorescence of tryptophan and tyrosine residues (Fig. 3). However, it should be noted that the emission spectrum of NPs appears to be redshifted and less intense when compared with the spectrum of α-LA in solution; these differences in fluorescence properties are indicative of sound changes in the environment of aromatic residues that occur during the assembly process. Specifically, the aforementioned spectral redshift suggests that aromatic residues are more exposed to the aqueous solvent in NPs than in native α-LA [28].

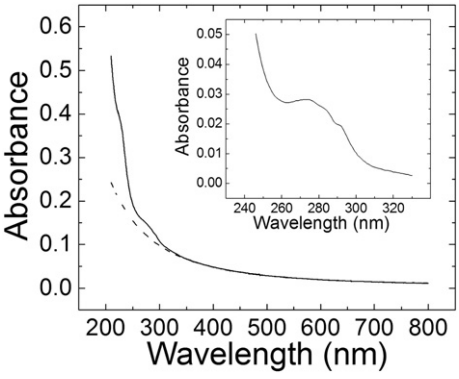

Fig. 1. Absorbance spectrum of α-lactalbumin nanoparticles (NPs) prepared by desolvation in acetone and cross-linking with glutaraldehyde. Solid line, spectrum of NPs in suspension (pH 7.0, 25.0 °C); dotted line, light-scattering contribution to the experimental spectrum of NPs (see Experimental section). Shown in the inset is the spectrum that resulted when the scattering component was subtracted from the experimental spectrum.

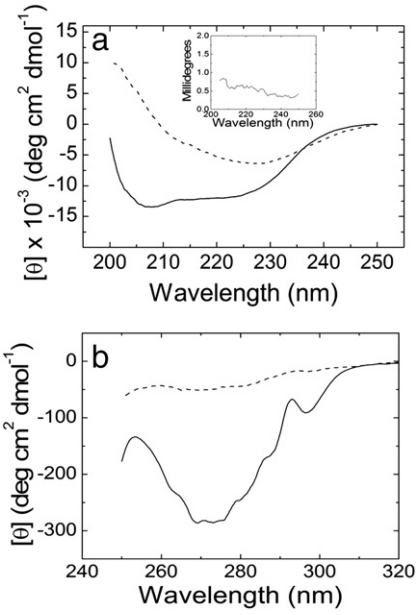

Fig. 2. Circular dichroism spectra of α-lactalbumin in its native form and as assembled into NPs. Far-UV (a) and near-UV (b) spectra of native (solid line) and assembled (dotted line) α-LA at pH 7.0 and 25.0 °C. Data are reported as mean residue ellipticity, [θ]. In panel (a), the inset shows the original ellipticity (in millidegrees) registered with a control sample of glutaraldehyde polymerized in acetone but in the absence of protein.

3.3. Effect of pH on the spectroscopic properties of α-LA nanoparticles

Spectroscopic studies were also carried out with NPs suspended in acidic (pH 3.0) and alkaline media (pH 9.0). As can be observed in Fig. 4a, variations in pH resulted in minor changes in the far-UV CD spectrum of NPs; the most conspicuous modification was related to the faint shoulder around 210 nm (wavelength that approximately corresponds to one minimum in the α-helix spectrum [25]), which is slightly enhanced at pH 9.0 but appears to be lost at pH 3.0. Nevertheless, results from spectral analysis indicate a hardly significant 2% increase in α-helix when the pH was varied from 3.0 to 9.0 (Table 1).

Likewise, pH-induced changes in the intrinsic-fluorescence intensity of NPs were rather minimal (Fig. 3). However, the emission band appears slightly redshifted at pH 9.0 with respect to pH 7.0, whereas at pH 3.0 the band loses definition and it is seen as a broad shoulder.

3.4. Size and polydispersity of α-LA nanoparticles

Electron micrographs (Fig. 5a) confirmed the spheroidal shape previously reported for α-LA NPs and their approximate diameters, which varied between 100 and 160 nm [15]. In contrast, polymerization of glutaraldehyde in the absence of protein produced particles of irregular shape and smaller dimensions (Fig. S1). DLS measurements carried out with NPs in suspension (pH 7.0) showed monomodal size distributions

Table 1
Fraction of secondary structure of α-lactalbumin before and after assemblage in nanoparticles.

Sample	α-Helix	β-Strands	Random
α-Lactalbumin (pH 7.0)	0.29	0.15	0.57
NPs (pH 7.0)	0.03	0.50	0.47
NPs (pH 9.0)	0.04	0.49	0.47
NPs (pH 3.0)	0.02	0.51	0.47

Determined by deconvolution of circular dichroism spectra using K2D algorithm (Dichroweb© 2013).

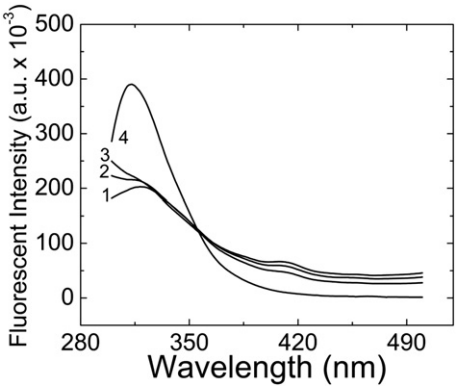

Fig. 3. Intrinsic fluorescence of α-LA nanoparticles at pH 9.0 (curve 1), 7.0 (curve 2), and 3.0 (curve 3); curve 4 is the spectrum of native α-LA at pH 7.0. In all cases, samples were excited with UV light of 280 nm.

(Fig. 5c), with a mean hydrodynamic diameter of 184 nm; a 0.07 polydispersity-index value indicated a relatively narrow width of distribution. Nonsignificant differences in diameter and polydispersity were found at the other pH values studied (results not shown).

3.5. Thermal stability of α-LA nanoparticles

DSC traces of dispersed NPs (pH 7.0) exhibited a broad endothermic transition (curve 2 in Fig. 6) accompanied by a large increase in the permanent heat capacity, ΔC_p, as indicated by the difference between the C_p values in the post- and the pretransition temperature regions. In comparison, control samples of glutaraldehyde polymerized in the absence of protein gave essentially flat DSC traces (results not shown). The lack of any endothermic effect in rescans of the NPs samples previously denatured in a first temperature scan (see dashed line in Fig. 6) indicated that the denaturation process was irreversible. Furthermore, the electron micrographs of nanoparticles that had been subjected to a calorimetric scan revealed the presence of entangled aggregates of somewhat distorted particles (Fig. 5b). Likewise, DLS measurements showed distributions with average sizes of approximately 700 nm for *temperature-denatured* nanoparticles (Fig. 5c). These observations suggest that the NP endotherm is in fact reflecting structural changes in the α-LA incorporated into the NPs, changes that lead to nanoparticle distortion and aggregation.

Although the endothermic nature of the transition and positive ΔC_p are properties that the nanoparticle suspension have in common with typical globular proteins [29,30], such as α-LA itself, it is evident from Fig. 6 that the heat absorbed during the transition (i.e., the area under the C_p curve spanning the transition) is smaller for NPs than for native α-LA (cf. curves 1 and 2 in Fig. 6). Indeed, the denaturation enthalpy, ΔH_d, for α-LA was determined as 17 ± 1 J/g, which is similar to previously reported values [27]. In contrast, the ΔH_d value for NPs amounted to only 7 ± 2 J/g (on a protein mass basis).

As can be observed in Fig. 6, DSC curves obtained at pH 9.0 were similar to those recorded at pH 7.0; likewise, ΔH_d determinations at both pH values were also alike (7 vs. 5 J/g). However, at pH 3.0, the endothermic transition was scarcely visible (Fig. 6, curve 4) and appeared displaced toward lower temperatures. Such a distinct thermal behavior for NPs at a low pH was also evident in far-UV CD spectra registered at 90 °C: in acidic media, the low- and high-temperature spectra were nearly identical, whereas at pH 7.0 and 9.0, the ellipticity measured below 220 nm became more negative upon heating to high temperature (Fig. 4b).

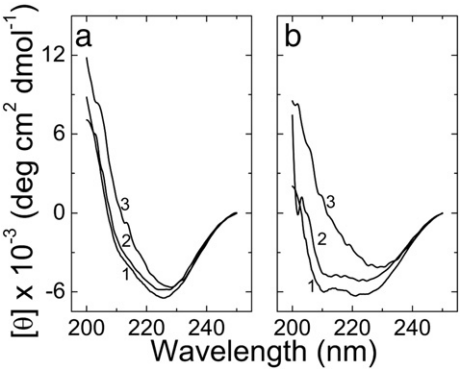

Fig. 4. Far-UV CD spectra of α-LA nanoparticles at 25.0 °C (a) and 90.0 °C (b). Spectra were registered at three pH values: 9.0 (curve 1), 7.0 (curve 2), and 3.0 (curve 3).

3.6. Effect of the protein–glutaraldehyde ratio on nanoparticle properties

Further studies were carried out to examine the influence of the protein to cross-linking agent ratio on the assembly of nanoparticles. For this purpose, a series of experiments were performed by following the standard procedure used to prepare NP samples in which the amount of glutaraldehyde was reduced. We found that halving the cross-linker concentration led to an increase of ca. 40% in the amount of assembled α-LA, whereas the size of the nanoparticles and properties of the incorporated protein remained like those observed for NPs (see Fig. S2). However, when lower concentrations of glutaraldehyde were used (one tenth or less of the original concentration) aggregates were mainly observed with a few NPs of smaller size (Fig. S3); moreover, the amount of α-LA incorporated in these samples was approximately ten-fold reduced with respect to the original samples. Finally, when native α-LA was cross-linked (no acetone added), oligomers no larger than 50 nm were obtained, and the secondary structure of the protein therein contained was rather similar to that of native α-LA as indicated by far-UV CD spectra (Fig. S4).

4. Discussion

4.1. Content and structure of α-LA in nanoparticles

We have applied spectroscopic and calorimetric methods to determine the basic structural characteristics of cross-linked α-LA that is incorporated in nanoparticles of a well-defined size. Because these methods require precise knowledge of the protein concentration to give meaningful results, the amount of α-LA present in the nanoparticle suspensions was quantified by directly assaying the total nitrogen (Kjeldahl method). The protocol based on the bicinchoninic acid (BCA) reagent, which is commonly used in biochemical work, was also used for protein determinations. Both of these methods provided similar, reproducible results. Strikingly, it was found that only ca. 4% of solid material in the nanoparticles came from the protein, although 54% of the total α-LA used for cross-linking was assembled. By doubling the protein/glutaraldehyde ratio, we could increase the yield of the assembled protein to 76% without affecting the morphology and stability of the resulting nanoparticles; however, the protein weight still represented a small fraction of the nanoparticle material (6 wt.%). Such a modest protein content in NPs is roughly consistent with the magnitude of UV-absorption bands (274–291 nm) after correction for light scattering (Fig. 1).

Hence, it is evident that α-LA nanoparticles are mainly composed of polymerized glutaraldehyde [31]. Nonetheless, the small amount of protein assembled appears to be necessary to form NPs of 100–160 nm in diameter (Fig. 5) because in the absence of α-LA glutaraldehyde polymerizes producing smaller particles with irregular shape (Fig. S1).

As reported in the literature [5,9,12], the optimization of the process for nanoparticle assembly involves the selection of an adequate pH at which there is net repulsion between protein molecules, and the right

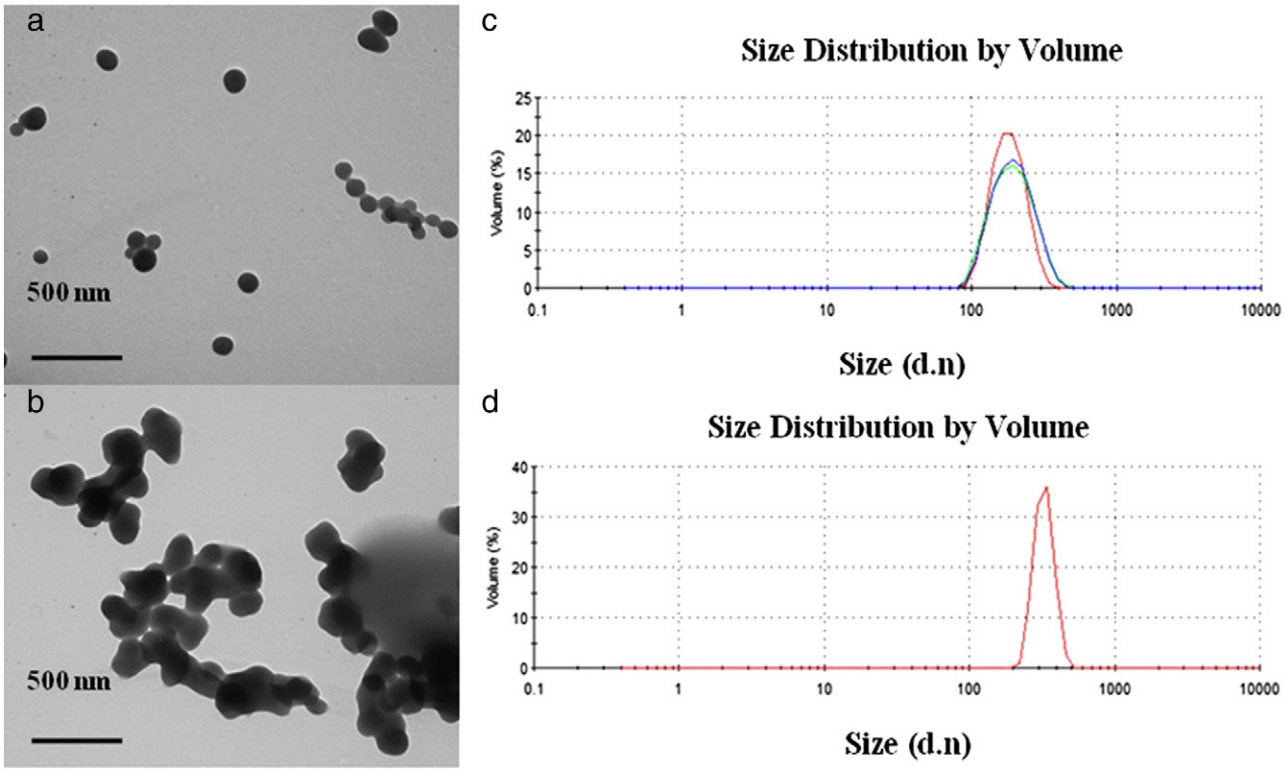

Fig. 5. Morphology and size of α-LA NPs. TEM images before (a) and after (b) thermal scanning in a DSC experiment. Size distribution by DLS of α-LA NPs before (c) and after (d) DSC experiment.

concentration of desolvating agent. Organic solvents that have been used for desolvation (i.e., acetone, ethanol, and isopropanol) are thought to decrease intermolecular hydrophobic interactions that can lead to the formation of bulky protein aggregates. On the other hand, it is well-known that organic solvents, when present at high concentrations, promote large conformational changes in proteins because they affect the hydrophobic effect that contributes to the stability of the native macromolecule [18,19]. This scenario is likely the case of α-LA treated with 80% acetone that was added prior to cross-linking. Indeed, as judged from far-UV CD spectra of NPs (Fig. 4), the assembled protein displays a β-strand-like conformation with virtually no helical regions that markedly differs from the predominantly helical secondary structure of native α-LA. It is clear that acetone brought about this large conformational change because the secondary structure of α-LA was affected to a lesser degree when cross-linking was performed with no previous desolvation treatment. In addition, this nonnative form of assembled α-LA lacks near-UV CD bands, indicating that its tyrosine and tryptophan side chains have lost their native asymmetric environment [32]. Besides, the Trp residues seem to be more exposed to the aqueous solvent than in native α-LA, as the fluorescence redshifts in Fig. 3 suggest [28].

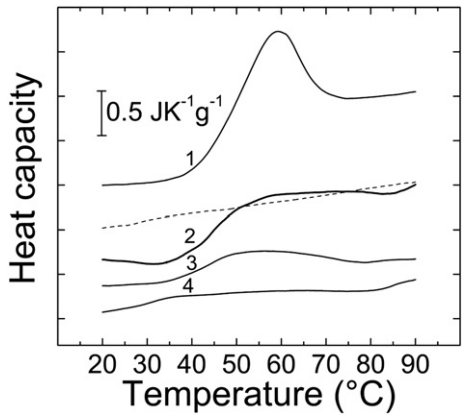

Fig. 6. DSC profiles of α-LA in its native form and as assembled into NPs. Curve 1, native protein at pH 7.0; curves 2, 3, and 4 are traces obtained with nanoparticles suspended in buffers of pH 7.0, 9.0, and 3.0, respectively. The dotted line is the second scan of the experiment shown in curve 2 (pH 7.0). All samples were scanned at 1.0 °C min^{-1}.

It is important to note that the polypeptide structure achieved within the nanoparticle assemblage is drastically distinct from the structure found in α-LA molten-globule states. These expanded forms of the protein, which are well-populated at acidic pH [27,33] or in the presence 0.50 M hexafluoroisopropanol (HFIP) [19], are characterized by a completely disrupted tertiary structure, but otherwise possess a high content of α-helix [27,34]. Interestingly, the secondary conformation of assembled α-LA and its denatured form in HFIP (alcohol concentration of 1.0 M or higher) may resemble each other, as suggested by the similar shape of their far-UV CD spectra. Taking the above evidence into account, the acetone-induced denaturation of α-LA seemingly results in an extended polypeptide structure in which many of its side chains might become available for reaction with glutaraldehyde. This reagent can react not only with amines but also with several other functional groups of proteins, such as guanidinyl, hydroxyl, and imidazole [31]. Thus, the large number of sites within a single polypeptide chain that may serve as cross-linking points, together with the polymeric nature of the reactive glutaraldehyde species that are known to exist in solution [31], may explain the low weight fraction of α-LA found in NPs.

4.2. Stability of assembled α-LA

Even though covalent bonds likely constitute a primary source of stability for α-LA nanoparticles, secondary (i.e., noncovalent) interactions also appear to play a role in this regard, as the DSC results point out. Specifically, the broad endothermic transition observed in calorimetric scans (Fig. 6) occurs at temperatures below 90 °C and under

pH conditions (3.0 to 9.0) that can hardly affect the integrity of covalent bonds. Rather, the endothermic effect reflects the breakdown of hydrogen bonds, van der Waals, and electrostatic interactions, as is the case with proteins that are subjected to similar ranges of temperature increments [35]. Accordingly, it seems that α-LA nanoparticles possess some degree of internal packing (i.e., nonsolvated regions stabilized via noncovalent interactions between different atomic groups). The large increase in C_p observed on up-temperature scans (Fig. 6) supports the proposal that inner nanoparticle regions of nonpolar nature become exposed to water at temperatures ca. 90 °C. It must be recognized, however, that the packing density in an α-LA nanoparticle should be less than in a globular protein molecule, as judged from the low ΔH_d value associated with the endothermic transition exhibited by NPs. The CD spectra registered at pH 7.0 and 90 °C (Fig. 4) clearly show that the heat-absorption effect is accompanied by changes in the polypeptide secondary structure. Electron micrographs provide further evidence for the stabilizing role played by noncovalent interactions because the NPs appeared deformed and were prone to aggregation (Fig. 5) after being subjected to thermal scanning, although their individual character was not completely lost.

With regard to the influence of pH on stability, the spectroscopic probes used in this study revealed that the overall structure of assembled α-LA undergoes only minor changes within the 3.0–9.0 pH interval at 25 °C (see Figs. 3 and 4). Similarly, the size distribution and average diameter of NPs appeared to be preserved throughout this pH range (results not shown). In contrast, DSC runs showed that the endotherm, which is clearly visible at pH 7.0 and 9.0, is barely discernible and shifted toward lower temperatures at pH 3.0. This suggests that limited regions within NPs are destabilized when the pH is brought to 3.0, whereas most of the inner structure actually becomes more resistant on up-temperature scans. In agreement with this view, CD spectra point out that the polypeptide conformation of assembled α-LA appears to be refractory to high temperatures at pH 3.0 (cf. low- and high-temperature CD spectra shown in Fig. 4). Undoubtedly, the pH effect that was just mentioned is linked to the (partial) protonation of carboxylates (intrinsic pK_a values from 4.0 to 4.5), and its physical background probably involves a shift in the balance between electrostatic interactions and hydrogen bonds. However, further studies are needed to clarify these issues.

5. Conclusions

Spherical nanoparticles (NPs) of 100–160 nm in diameter comprising α-LA cross-linked with glutaraldehyde in the presence of acetone (80% v/v) were studied to determine the structure of the embedded protein and its amount relative to the cross-linking agent. Direct protein quantification revealed that assembled α-LA contributes only 4% of the nanoparticle dry weight. Even though NPs are predominantly formed by polymerized glutaraldehyde, the small amount of protein incorporated appears to be necessary to obtain NPs on the hundred-nanometer scale. Owing to the denaturing effect of acetone, the polypeptide chain of assembled α-LA acquires a β-strand-like conformation, which is devoid of the tertiary structure typical of the native protein. It is then proposed that as a result of acetone-induced denaturation, multiple α-LA side chains become available for reaction with polymeric forms of glutaraldehyde, thus explaining the low protein weight fraction found in NPs.

Although much of the nanoparticle stability is due to covalent bonds, noncovalent interactions seemingly impart additional stability to the assemblage. At low temperatures, neither the nanoparticle morphology nor the conformation of assembled α-LA is significantly affected by changes in the 3.0–9.0 pH region. However, the behavior of NPs on temperature scans was distinctly different at low pH; specifically, the major part of the nanoparticle structure apparently becomes refractory to high temperatures at pH 3.0. This result suggests that carboxylate group protonation shifts the balance between stabilizing and destabilizing noncovalent interactions.

Notes

The authors declare no competing financial interest.

Acknowledgment

This work was funded in part by the CONACYT, Mexico (SEP-CONACYT 2007-80457) and ICYTDF, Mexico (ICYTDF BI12-121). I. A.-M. thanks the CONACYT, Mexico (Registration no. 208139) for financial support. We would like to thank María Esther Sánchez-Espíndola (Instituto Politécnico Nacional) for her help in performing TEM experiments.

Appendix A. Supplementary data

Additional TEM micrographs (S1: polymerized glutaraldehyde, S2 and S3: NPs prepared by means of reducing glutaraldehyde concentration, and S4: NPs obtained from non-desolvated α-LA). Supplementary data to this article can be found online at http://dx.doi.org/10.1016/j.bpc.2014.07.003.

References

[1] M. Jahanshahi, Z. Babaei, Protein nanoparticle: a unique system as drug delivery vehicles, Afr. J. Biotechnol. 7 (2008) 4926–4934.
[2] J. Weiss, P. Thakistov, D.J. McClements, Functional materials in food nanotechnology, J. Food Sci. 71 (2006) 107–116.
[3] J.K. Momin, C. Jayakumar, J.B. Prajapati, Potential of nanotechnology in functional foods, Emir. J. Food Agric. 25 (2013) 10–19.
[4] Q. Huang, H. Yun, Q. Ru, Bioavailability and delivery of nutraceuticals using nanotechnology, J. Food Sci. 75 (2010) 50–57.
[5] S. Gunasekaran, S. Ko, L. Xiao, Use of whey proteins for encapsulation and controlled delivery applications, J. Food Eng. 83 (2007) 31–40.
[6] L. Chen, G.E. Remondetto, M. Subirade, Food protein-based materials as nutraceutical delivery systems, Trends Food Sci. Technol. 17 (2006) 272–283.
[7] S. Neethirajan, D.S. Jayas, Nanotechnology for the food and bioprocessing industries, Food Bioprocess Technol. 4 (2011) 39–47.
[8] M. Cushen, J. Kerry, M. Morris, M. Cruz-Romero, E. Cummins, Nanotechnologies in the food industry — recent developments, risks and regulation, Trends Food Sci. Technol. 24 (2012) 30–46.
[9] K. Langer, S. Balthasar, V. Vogel, N. Dinauer, H. von Briesen, D. Schubert, Optimization of the preparation process for human serum albumin (HAS) nanoparticles, Int. J. Pharm. 257 (2003) 169–180.
[10] W. Lin, A.G.A. Coombes, M.C. Garnett, M.C. Davies, E. Schacht, S.S. Davis, L. Illum, Preparation of sterically stabilized human serum albumin nanospheres using a novel Dextranox-MPEGP crosslinking agent, Pharm. Res. 11 (1994) 1588–1592.
[11] J. Kreuter, Nanoparticles—a historical perspective, Int. J. Pharm. 331 (2007) 1–10.
[12] C. Weber, C. Coester, J. Kreuter, K. Langer, Desolvation process and surface characterization of protein nanoparticles, Int. J. Pharm. 194 (2000) 91–102.
[13] A. Bansal, D.N. Kapoor, R. Kapil, N. Chhabra, S. Dhawan, Design and development of placlitaxel-loaded bovine serum albumin nanoparticles for brain targeting, Acta Pharma. 61 (2011) 141–156.
[14] R. Mehravar, M. Jahanshahi, N. Saghatolerlami, Production of biological nanoparticles from α-lactalbumin for drug delivery and food science application, Afr. J. Biotechnol. 8 (2009) 6822–6827.
[15] I.J. Arroyo-Maya, J.O. Rodiles-López, M. Cornejo-Mazón, G.F. Gutiérrez-López, A. Hernández-Arana, C. Toledo-Núñez, H. Hernández-Sánchez, Effect of different treatments on the ability of α-lactalbumin to form nanoparticles, J. Dairy Sci. 95 (2012) 6204–6214.
[16] B. Storp, A. Engel, A. Boeker, M. Ploeger, K. Langer, Albumin nanoparticles with predictable size by desolvation procedure, J. Microencapsul. 29 (2012) 138–146.
[17] K.S. Soppimath, T.M. Aminabhavi, A.R. Kulkarni, W.E. Rudzinski, Biodegradable polymeric nanoparticles as drug delivery systems, J. Control. Release 70 (2001) 1–20.
[18] K. Griebenow, A.M. Klivanov, On protein denaturation in aqueous–organic mixtures but not in pure organic solvents, J. Am. Chem. Soc. 118 (1996) 11695–11700.
[19] A. Kundo, N. Kishore, 1,1,1,3,3,3-Hexafluoroisopropanol induced thermal unfolding and molten globule state of bovine α-lactalbumin: calorimetric and spectroscopic studies, Biopolymers 73 (2004) 405–420.
[20] J.J. Marty, R.C. Oppenheim, P. Speiser, Nanoparticles—a new colloidal drug delivery system, Pharm. Acta Helv. 53 (1978) 17–23.
[21] AOAC, Official Methods of Analysis of Official Analytical Chemists, 15th ed, 342, AOAC International, Washington, DC, 1990, (1095, 1096, 1105, 1106).
[22] P.K. Smith, R.I. Krohn, G.T. Hermanson, A.K. Mallia, F.H. Gartner, M.D. Provenzano, E. K. Fujimoto, N.M. Goeke, B.J. Olson, D.C. Klenk, Measurement of protein using bicinchoninic acid, Anal. Biochem. 150 (1985) 76–85.
[23] J.Z. Porterfield, A. Zlotnick, A simple and general method for determining the protein and nucleic acid content of viruses by UV absorbance, Virology 407 (2010) 281–288.
[24] P. Manavalan, W.C. Johnson, Sensitivity of circular dichroism to protein tertiary structure class, Nature 305 (1983) 831–832.

[25] W.C. Johnson Jr., Protein secondary structure and circular dichroism: a practical guide, Proteins Struct. Funct. Genet. 7 (1990) 205–214.
[26] K. Matsuo, Y. Sakurada, S. Tate, H. Namatame, M. Taniguchi, K. Gekko, Secondary-structure analysis of alcohol-denatured proteins by vacuum-ultraviolet circular dichroism spectroscopy, Proteins 80 (2012) 281–293.
[27] V.Y. Grinberg, N.V. Grinberg, T.V. Burova, M. Dalgalarrondo, T. Haertle, Ethanol-induced conformational transitions in holo-α-lactalbumin: spectral and calorimetric studies, Biopolymers 46 (1998) 253–265.
[28] I.D. Campbell, R.A.R. Dwek, Biological Spectroscopy, The Benjamin/Cummings Publishing Company, Inc, Menlo Park, CA, 1984.
[29] P.L. Privalov, Stability of proteins: small globular proteins, Adv. Protein Chem. 33 (1979) 167–241.
[30] A.D. Robertson, K.P. Murphy, Protein structure and the energetics of protein stability, Chem. Rev. 97 (1997) 1251–1268.
[31] I. Migneault, C. Dartiguenave, M.J. Bertrand, K.C. Waldron, Glutaraldehyde: behavior in aqueous solution, reaction with proteins, and application to enzyme crosslinking, BioTechniques 37 (2004) 790–802.
[32] H. Strickland, J. Horwitz, C. Billups, Analysis of vibrational structure in the near-ultraviolet circular dichroism and absorption spectra of phenylalanine and its derivatives, J. Am. Chem. Soc. 91 (1969) 184–190.
[33] Y.V. Griko, E. Freire, P.L. Privalov, Energetics of the alpha-lactalbumin states: a calorimetric and statistical thermodynamic study, Biochemistry 33 (1994) 1889–1899.
[34] M. Nozaka, K. Kuwajima, K. Nitta, S. Sugai, Detection and characterization of the intermediate on the folding pathway of human alpha-lactalbumin, Biochemistry 17 (1978) 3753–3758.
[35] G.I. Makhatadze, P.L. Privalov, Energetics of protein structure, Adv. Protein Chem. 47 (1995) 307–425.